*Romanian Reports in Physics, Vol. 59, No. 2, P. 261–271, 2007*

*Dedicated to Prof. Dorin N. Poenaru's 70th Anniversary*

# SELECTED EFFECTS OF THE IN-MEDIUM NUCLEON-NUCLEON CROSS SECTION ON HEAVY-ION DYNAMICS BELOW 100 MeV/$u$

Z. BASRAK[1], Ph. EUDES[2], F. SÉBILLE[2]

[1]*Ruđer Bošković Institute, P.O. Box 118, HR-10 002 Zagreb, Croatia*
*E-mail: basrak@irb.hr*
[2]*SUBATECH, EMN-IN2P3/CNRS-Université de Nantes, P.O. Box 20722*
*F-44307 Nantes cedex 3, France, E-mail: eudes@subatech.in2p3.fr*

(Received February 15, 2007)

*Abstract.* The role of the value of the in-medium nucleon-nucleon cross section on nuclear dynamics at intermediate energies is studied within the framework of a semiclassical transport model. Particular attention is payed to the early reaction phase and the effects produced on the energy transformed into heat and compression as well as on the prompt dynamical emission.

*Key words:* heavy-ion reactions, semiclassical transport model, in-medium cross-section.

## 1. **INTRODUCTION**

Despite of many decades of theoretical and experimental efforts, the question of nuclear equation of states (EOS) is still open. With time it has become increasingly evident that the EOS cannot be studied separately from the unresolved question of a possible contribution of nuclear surroundings to the elementary particle scattering even at energies below 100 MeV/nucleon where inelastic processes are negligible. Nevertheless, the effects of the in-medium modified nucleon-nucleon ($NN$) scattering probability on heavy-ion dynamics have so far been rarely studied in detail.

In the present work we systematically investigate the effects of the $NN$ scattering cross section on several dynamical observables of interest for heavy-ion reactions (HIR). We use the Landau-Vlasov (LV) model [1], an one-body

microscopic transport approach complemented with the two-body correction term (Boltzmann's collision integral), which is reputed to correctly describe the bulk properties of HIR at intermediate energies. The LV equation describes the spatio-temporal evolution of the distribution function $f(\mathbf{r},\mathbf{p};t)$ under the mean field hamiltonian $H$ of nuclear and Coulomb origin

$$\frac{\partial f(\mathbf{r},\mathbf{p};t)}{\partial t} + \{f(\mathbf{r},\mathbf{p};t), H\} = I_{\rm coll}(f(\mathbf{r},\mathbf{p};t)). \tag{1}$$

The symbol $\{\ ,\ \}$ stands for the Poisson brackets. The collision integral is calculated in the Uehling-Uhlenbeck approximation [2]

$$\begin{aligned} I_{\rm coll} \;=\; & \frac{g}{4m^2}\;\frac{1}{\pi^3\hbar^3}\int d\mathbf{p_2}\; d\mathbf{p_3}\; d\mathbf{p_4}\;\frac{d\sigma^{\rm m}_{\rm NN}}{d\Omega} \\ & \times\; \delta(\mathbf{p}+\mathbf{p_2}-\mathbf{p_3}-\mathbf{p_4})\;\delta(\epsilon+\epsilon_2-\epsilon_3-\epsilon_4) \\ & \times\; [(1-\bar{f})(1-\bar{f}_2)f_3f_4-(1-\bar{f}_3)(1-\bar{f}_4)f_2f]\;, \end{aligned} \tag{2}$$

and takes into account energy and momentum conservation as well as the Pauli exclusion principle. The symbol $g$ is the degeneracy, $m$ is the nucleon mass, $\bar{f}=(2\pi\hbar)^3 f(\mathbf{r},\mathbf{p};t)/g$ is the occupation number, $\mathbf{p}$ and $\mathbf{p_2}$ ($\mathbf{p_3}$ and $\mathbf{p_4}$) are initial (final) momenta of the scattering particle pair, $\epsilon=\epsilon(p)$ is the single-particle energy, while $\sigma^{\rm m}_{\rm NN}$ is the *in-medium* transition probability defined as

$$\sigma^{\rm m}_{\rm NN} = F\,\sigma^{\rm f}_{\rm NN}. \tag{3}$$

Here $\sigma^{\rm f}_{\rm NN}$ is the *free* $NN$ cross section with its usual energy and isospin dependence and $F$ is a corrective constant factor. For the sake of simplicity, $\sigma^{\rm f}_{\rm NN}$ is assumed to be isotropic and density independent, an approximation which is fully justified in HIR below 100 MeV/$u$. Equation (1) is solved numerically in the Wigner representation for a nonlocal effective force (Gogny D1–G1, the incompressibility modulus $K_\infty = 228$ MeV, and the effective mass $m^*/m = 0.67$ [3]) by projecting the one-body nuclear phase space onto a continuous basis of thousands of coherent states (here 100 per nucleon) taken as elementary Gaussian functions [4]. The LV model with the Gogny interaction generates a well-defined mean field with a proper surface dependence and includes the Coulomb interaction, which is essential at low incident energies.

From the technical point of view, as in any Monte-Carlo-method based calculation, the quality of the used random number generator is of a fundamental meaning. The presented results are the first LV model simulations obtained with a true quantum random bit generator [5] and not with a classical pseudorandom number generator.

In this paper we present the results on the study of the $^{36}$Ar+$^{58}$Ni and $^{58}$Ni+$^{58}$Ni reactions at 52, 74, and 95 MeV/$u$ (52, 74, and 90 MeV/$u$ for the latter reaction) at all impact parameters from central to peripheral collisions. These systems have been extensively studied experimentally by the INDRA

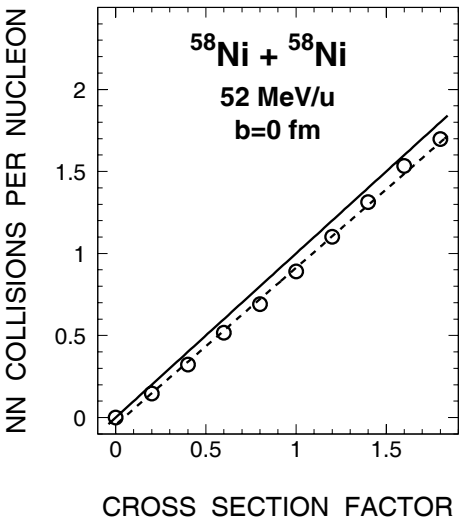


Fig. 1 – The number of $NN$ collisions in the system, accumulated between the instant $t$=0 of the contact of colliding nuclei and the instant $t_{\rm sep}$ (see text for the definition), divided by the number of nucleons bound within the QP and QT at $t_{\rm sep}$ as a function of the multiplicative factor $F$ of eq. (3). Shown is the result for the $^{58}$Ni+$^{58}$Ni system at 52 MeV/$u$ in the head-on collision. The dotted line is the best-fit result, while the full line displays the bisectrix $y = x$.

collaboration at GANIL [6, 7, 8]. Although in some publications the multiplicative factor $F$ of eq. (3) was varied between 0.5 and 5 (see, e.g. [9]), the motivation for such extreme values was solely in demonstrating their nonphysical character and a large discrepancy of such a prediction from experimental reality. In the present study, $F$ takes the values 0.8, 1, 1.2, and 1.5.

## 2. EARLY ENERGY TRANSFORMATION

In central nucleus-nucleus collisions stopping is mainly due to the viscous feature of nuclear fluid. The nuclear viscosity from around the Fermi energy upward receives contribution not only from the one-body (mean-field) component, but increasingly also a contribution coming from the two-body ($NN$) dissipation of the initial motion. An expected trivial result is that, on the average, the number of $NN$ collisions per nucleon is proportional to $\sigma_{\rm NN}^{\rm m}$. Indeed, as shown in Fig. 1, the average number of hard $NN$ collisions per nucleon almost perfectly follows the $y = x$ bisectrix line.

It has recently been shown theoretically [10, 11, 12] and confirmed experimentally [8] that HIR at intermediate energies, especially for central collisions, are strongly dominated by the midrapidity emission, a component which

is emitted early during the dynamical reaction phase. As an example, Fig. 2 shows the emission rate of the Ni+Ni reaction in a central and a peripheral collision. In both cases, the emission pattern displays a copious dynamical contribution from the first compact reaction stage which may be considered to cease at the instant $t_{\rm sep}$ (labeled by heavy vertical bars in Fig. 2) at which the quasiprojectile (QP) and quasitarget (QT) emerge and separate in the exit reaction channel. The rest of the abundant emission is due to the rupture of the so-called neck which is formed between QP and QT. This shortly lasting emission is followed by a typical calm statistical-like disintegration by which moderately hot QP and QT cool down slowly [12, 13]. This prompt and copious dynamical emission (DE) from the first compact reaction stage is proportional to the impact parameter $b$, i.e., to the reaction geometry [10, 11, 13]. We underline that the physical nature of the DE component is different from the relatively well-studied neck-rupture mechanism by which the midrapidity domain is also fed. Most of the studies of the neck-rupture are devoted to semiperipheral collisions, in which this component may be distinguished by higher clustering probability. For a review of semiperipheral studies, see the most recent experimental [7, 14, 15] and theoretical works [16, 17].

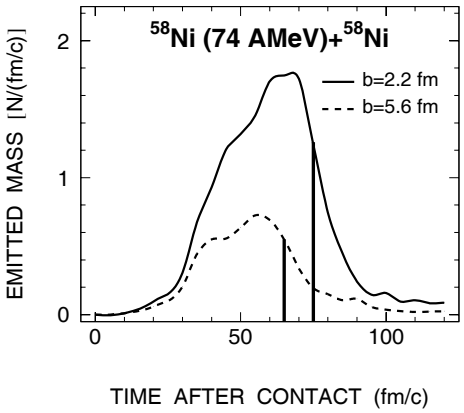


Fig. 2 – Time evolution of the nucleon emission rate for the Ni+Ni reaction at 74 MeV/$u$ and a central and a peripheral impact parameter. The vertical bars label the instant $t_{\rm sep}$. The factor $F$ of eq. (3) is equal to one.

The prompt DE particles evacuate a large amount of available system energy. Since this emission occurs in the early compact phase of HIR, it is crucial to study details of the early transformation of the initial relative motion of the entrance reaction channel into other forms of energy. A quantitative study of the main energy components that are responsible for the observed copious midrapidity emission, namely, heat and compression energy, has recently been reported [18]. Here, we investigate how the change of $\sigma_{\rm NN}^{\rm m}$ influences the early

energy transformation and, in particular, how heat and compression energy behave as a function of the factor $F$.

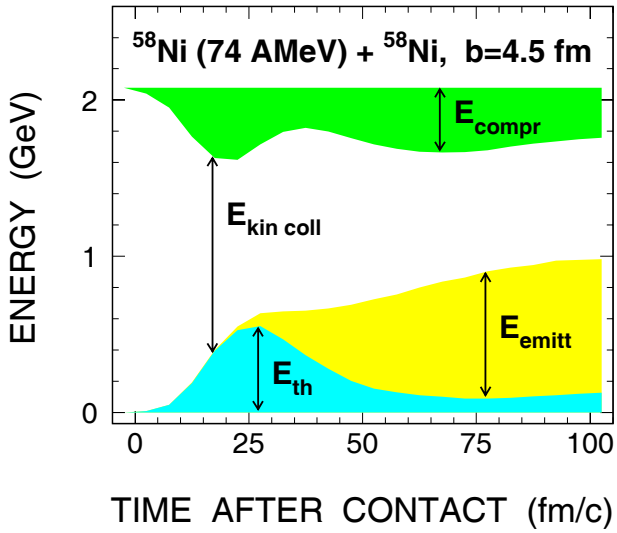


Fig. 3 – Time evolution of the energy components for the Ni+Ni reaction at 74 MeV/$u$ and an intermediate impact parameter. The available entrance channel energy in the center-of-mass is prior to the contact of colliding partners in the form of the kinetic energy of their relative motion. After the contact, this collective kinetic energy $E_{\mathrm{kin\ coll}}$ is rapidly transformed into the compression $E_{\mathrm{compr}}$ and the heat $E_{\mathrm{th}}$. Negligible at the beginning of the collision, the energy $E_{\mathrm{emitt}}$ carried out of the system by emitted particles, becomes the dominant energy component shortly after $E_{\mathrm{compr}}$ and $E_{\mathrm{th}}$ have passed their maxima. The factor $F$ of eq. (3) is equal to one.

The center-of-mass energy may be decomposed into collective and intrinsic contributions,

$$E_{\mathrm{tot}} = E_{\mathrm{coll}} + E_{\mathrm{int}}. \tag{4}$$

The component $E_{\mathrm{int}}$ may be further subdivided into the excitation energy contribution $E^*$ and the "cold" (potential) contribution which is evaluated in the Thomas-Fermi limit as is usual in semiclassical approaches. In the present study, instead of the common local sphere approximation the "cold" contribution is evaluated in the so-called local bisphere approximation which, in the zone of overlap of the two spheres at zero temperature, does not violate the Pauli principle [19]. Such a treatment is relevant even on the time scale on which the system is clearly out of equilibrium. This "cold" kinetic energy ($E_0$ in [19]) may, in the first approximation, be identified with the *compression* $E_{\mathrm{compr}}$. Strictly speaking, $E^*$ can be identified with thermal energy (heat) only at the limit when the pressure tensor is equilibrated, which does not occur for

the reaction time of interest in the present study. Nevertheless, for the didactic purpose, this proto-thermal component of the total energy is hereafter referred to as *thermal energy* $E_{\rm th}$ or *heat*. To summarize, one may write

$$E_{\rm int} = E_{\rm th} + E_{\rm compr} + E_{\rm emitt}, \tag{5}$$

where $E^* = E_{\rm th}$ and $E_{\rm emitt}$ is the energy evacuated from the system by particle emission.

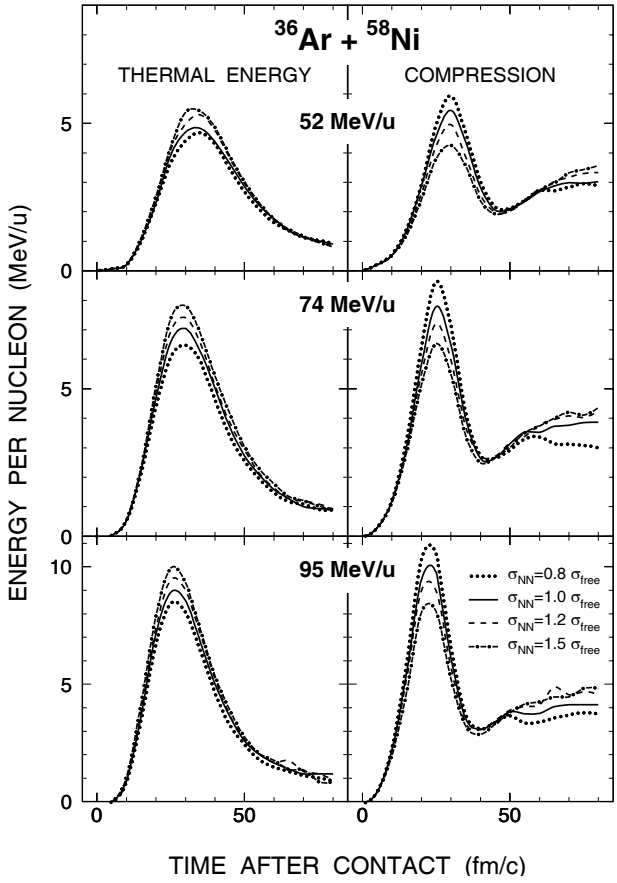


Fig. 4 – The thermal (left) and compression energy (right) per nucleon as a function of time and $\sigma_{\rm NN}^{\rm m}$ at 52 (top), 74 (middle), and 95 MeV/$u$ (bottom) in head-on collisions of $^{36}$Ar and $^{58}$Ni nuclei. Dotted curves are for $F = 0.8$, full for $F = 1$, dashed for $F = 1.2$, and dot-dashed for $F = 1.5$.

The collective contribution $E_{\rm kin\ coll}$ is defined in the usual way:

$$E_{\rm kin\ coll} = \frac{1}{2} \int d^3\mathbf{r}\, \frac{\mathbf{j}(\mathbf{r})^2}{\rho(\mathbf{r})}, \tag{6}$$

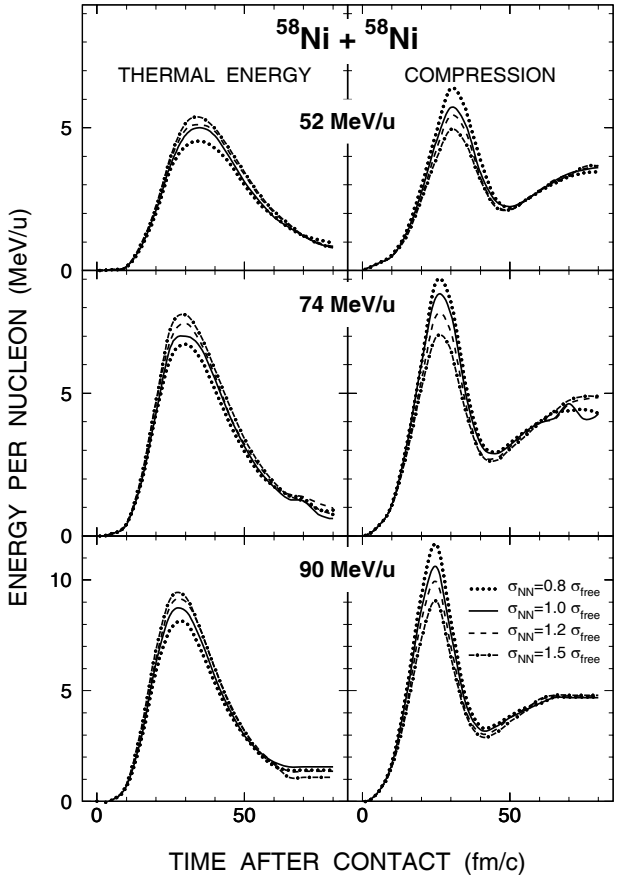


Fig. 5 – Same as Fig. 4 but for the $^{58}$Ni+$^{58}$Ni reaction.

i.e., at each instant of dynamics it is an integral over the whole system of the square of a local collective current $\mathbf{j} = \rho\mathbf{v}$ normalized by the local density $\rho$. For details see, e.g., Ref. [19]. A typical time evolution of the system energy is shown in Fig. 3.

The time evolution of heat and compression during the early dynamical reaction phase at three energies as a function of the factor $F$ is shown in Fig. 4 (Fig. 5) for the Ar+Ni (Ni+Ni) reaction in the head-on regime. For other impact parameters, the dependence on $\sigma_{\mathrm{NN}}^{\mathrm{m}}$ is weaker and vanishes for grazing collisions. Nevertheless, the dependence on the reaction geometry persists and is in full agreement with the study [18].

It is worth noting that $E_{\mathrm{th}}$ increases with $\sigma_{\mathrm{NN}}^{\mathrm{m}}$, whereas $E_{\mathrm{compr}}$ decreases. This is clearly visible in the behavior of the above energy components maxima shown in Fig. 6 for the Ni+Ni reaction. As expected, the value of the energy maxima increases with the entrance channel energy. The instant at which

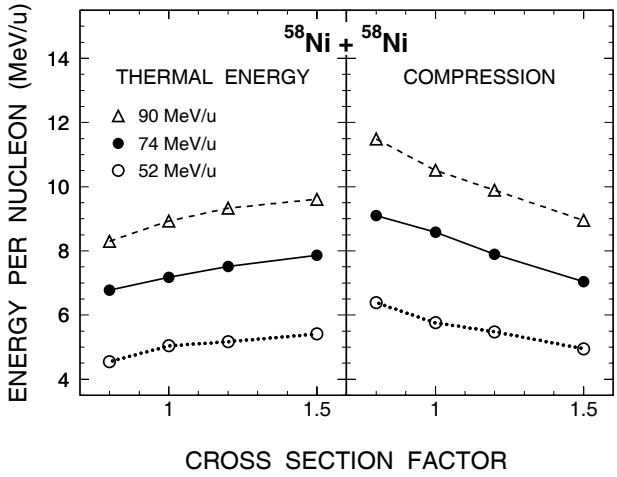


Fig. 6 – The value of thermal (left) and compression energy (right) maxima of Fig. 5 as a function of the factor $F$ of eq. (3) at 52 (open circles), 74 (full circles), and 90 MeV/$u$ (triangles).

these maxima are reached is almost independent of $\sigma_{\rm NN}^{\rm m}$ and decreases with increasing relative velocity of colliding nuclei, as shown in Fig. 7 for the Ar+Ni reaction. One also sees that $E_{\rm th}$ reaches its maximal value a few fm/$c$ before $E_{\rm compr}$ reaches its.

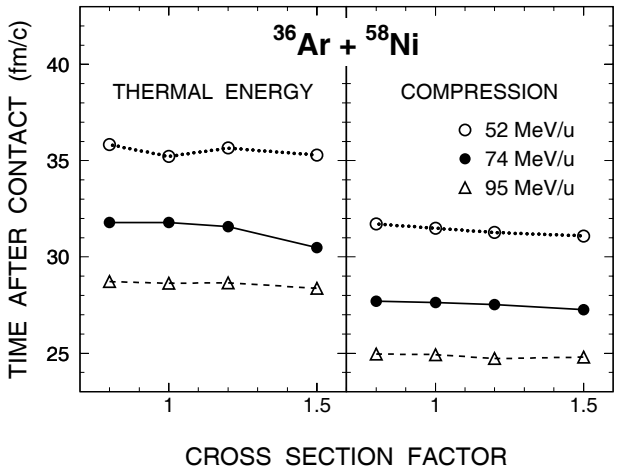


Fig. 7 – The instant at which the maximum of thermal (left) and compression energy (right) of Fig. 4 is reached as a function of the factor $F$ of eq. (3) at 52 (open circles), 74 (full circles), and 95 MeV/$u$ (triangles).

## 3. DYNAMICAL EMISSION

Dynamical emission (DE) was introduced in the preceding section. Since these particles are emitted during the early compact reaction phase, one expects that the value of $\sigma_{\rm NN}^{\rm m}$ has a strong impact onto DE. As in [11], we define the quantity

$$D_{\rm em} = 100\frac{\#DE}{Z_{\rm tot}}, \tag{7}$$

which corresponds to the amount of charged particles emitted before $t_{\rm sep}$ divided by the total charge of the system, $Z_{\rm tot} = Z_{\rm T} + Z_{\rm P}$, where the subscript T (P) stands for the target (projectile). $D_{\rm em}$ takes the value 0 % if no DE occurs, and 100 % if the whole system disintegrates by DE.

Figure 8 shows how DE depends on the reaction centrality as a function of $\sigma_{\rm NN}^{\rm m}$. As a reference, shown is a curve which represents the size of the overlapping region between the target and the projectile in a fully geometrical

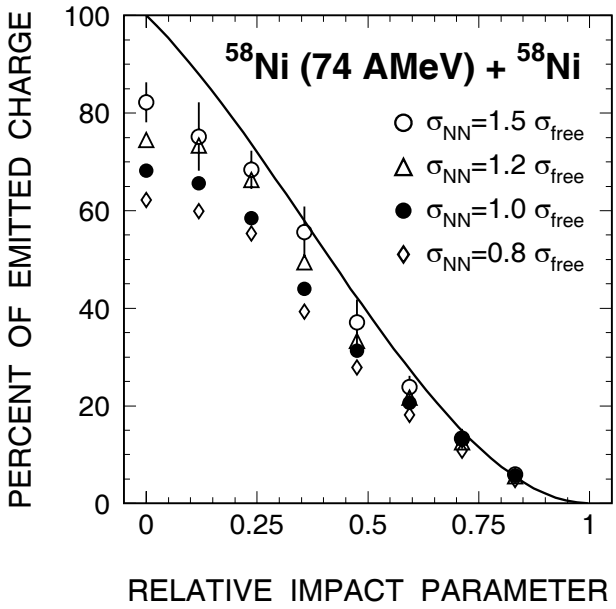


Fig. 8 – Simulation results for the evolution of dynamical emission as a function of the reduced impact parameter for the Ni+Ni reaction at 74 MeV/$u$ as a function of $\sigma_{\rm NN}^{\rm m}$. Different symbols used denote different values of $F$: circles for $F$=1.5, triangles $F$=1.2, filled circles $F$=1, and diamonds $F$=0,8. The curve is due to a simple estimate of the contribution of participant matter assuming a purely geometrical overlap of the two interpenetrating spheres [20] in the spirit of the participant-spectator picture [21].

assumption [20]. The centrality of the reaction is expressed via the reduced impact parameter, i.e., the impact parameter normalized according to $b_{\max} = R_{\mathrm{T}} + R_{\mathrm{P}}$, where $R_{\mathrm{T}}$ ($R_{\mathrm{P}}$) stands for the radius of the target (projectile). The values and the error bars reported in the figure correspond, respectively, to the mean value and the difference obtained by considering DE at $t_{\mathrm{sep}}$ and at $t_{\mathrm{sep}} + 5\,\mathrm{fm}/c$. For the sake of figure clarity, the error bars stand for the $F = 1.5$ case only, but they are essentially the same for other studied values of the factor $F$. Despite of somewhat scattered points, the value of DE is evidently proportional to the value of $\sigma_{\mathrm{NN}}^{\mathrm{m}}$. This observation may be used to constrain the factor by which the free $NN$ cross section $\sigma_{\mathrm{NN}}^{\mathrm{f}}$ has to be modified in order to account for the modifications of the elementary $NN$ scattering process caused by the presence of nuclear surroundings.

## 4. SUMMARY

To experimentally disentangle the contribution of the so-called nuclear EOS from the possible effects coming from the in-medium distortion of elementary free-particle scattering is an extremely difficult problem. The aim of the present work is to contribute to unraveling the very complex heavy-ion-reaction mechanisms in the intermediate energy regime by studying how the change in $\sigma_{\mathrm{NN}}$ affects the early reaction phase, in particular the thermal and compression energy and the so-called dynamical emission. The value of $\sigma_{\mathrm{NN}}^{\mathrm{m}}$ may also have consequences on the fusion disappearance [22], a phenomenon occurring around the Fermi energy. This work is in progress and will be reported elsewhere.

*Acknowledgements.* This work was supported in part by the Croatian Ministry of Science, Education and Sports, Grant No. 0098-1191005-2879.

## REFERENCES

1. C. Grégoire et al., Nucl. Phys., A **436**, 365 (1985).
2. L.W. Nordheim, Proc. Roy. Soc., **A119**, 689 (1928); E.A. Uehling and G.E. Uhlenbeck, Phys. Rev., **43**, 552 (1933).
3. J. Dechargé and D. Gogny, Phys. Rev., **C 21**, 1568 (1980).
4. B. Remaud, F. Sébille, C. Grégoire, L. Vinet, and Y. Raffray, Nucl. Phys., **A447**, 555c (1985); F. Sébille, G. Royer, C. Grégoire, B. Remaud, and P. Schuck, Nucl. Phys., **A501**, 137 (1989).
5. M. Stipčević, B. Medved Rogina, `http://arxiv.org/abs/quant-ph/0609043`; `http://qrbg.irb.hr`.

6. INDRA Collaboration, P. Lautesse *et al.*, Eur. Phys. J., A **27**, 349 (2006); INDRA Collaboration, P. Lautesse *et al.*, Phys. Rev., C **71**, 034602 (2005); INDRA Collaboration, J.D. Frankland *et al.*, Phys. Rev., C **71**, 034607 (2005); INDRA Collaboration, E. Galichet *et al.*, Eur. Phys. J., A **18**, 75 (2003); INDRA Collaboration, D. Cussol *et al.*, Phys. Rev., C **65**, 044604 (2002); INDRA Collaboration, P. Desesquelles *et al.*, Phys. Rev., C **62**, 024614 (2000); INDRA Collaboration, M.F. Rivet *et al.*, Phys. Lett., **B 388**, 219 (1996); INDRA Collaboration, B. Borderie *et al.*, Phys. Lett., **B 388**, 224 (1996); INDRA Collaboration, C.O. Bacri *et al.*, Phys. Lett., **B 353**, 27 (1995).
7. INDRA Collaboration, D. Thériault *et al.*, Phys. Rev., C **71**, 014610 (2005).
8. INDRA Collaboration, D. Doré *et al.*, Phys. Lett., **B 491**, 15 (2000); INDRA Collaboration, T. Lefort *et al.*, Nucl. Phys., **A 662**, 397 (2000); INDRA Collaboration, D. Doré *et al.*, Phys. Rev., C **63**, 034612 (2001).
9. FOPI Collaboration, B. Hong *et al.*, Phys. Rev., **C 66**, 034901 (2002).
10. Ph. Eudes, Z. Basrak, and F. Sébille, Phys. Rev., C **56**, 2003 (1997).
11. F. Haddad, Ph. Eudes, Z. Basrak, and F. Sébille, Phys. Rev., C **60**, 031603 (1999).
12. Ph. Eudes and Z. Basrak, in *Proceedings of the International Nuclear Physics Conference*, Paris, 1998, edited by B. Frois, D. Goutte, and D. Guillemaud-Mueller [Nucl. Phys., **A 654**, 769c (1999)].
13. Ph. Eudes and Z. Basrak, Eur. Phys. J., A **9**, 207 (2000).
14. E. De Filippo *et al.*, Phys. Rev., C **71**, 044602 (2005).
15. INDRA Collaboration, P. Lautesse *et al.*, Phys. Rev., C **71**, 034602 (2005).
16. V. Baran, M. Colonna, and M. Di Toro, Nucl. Phys., **A 730**, 329 (2004).
17. A. Chernomoretz *et al.*, Phys. Rev., C **65**, 054613 (2002).
18. I. Novosel, Z. Basrak, Ph. Eudes, F. Haddad and F. Sébille, Phys. Lett., **B 625**, 26 (2005).
19. P. Abgrall, F. Haddad, V. de la Mota, and F. Sébille, Phys. Rev., C **49**, 1040 (1994).
20. R.W. Hasse, W.D. Myers, *Geometrical Relationships of Macroscopic Nuclear Physics*, Springer Verlag, Berlin, 1970.
21. G.D. Westfall, *et al.*, Phys. Rev. Lett., **37**, 1202 (1976).
22. Z. Basrak and Ph. Eudes, in *Proceedings of the International Conference on Clustering Aspects of Nuclear Structure and Dynamics*, Rab, Croatia, 1999, edited by M. Korolija, Z. Basrak, and R. Čaplar, World Scientific, 2000, p. 316.